Published in final edited form as:
Exp Neurol. 2014 July ; 257: 170–181. doi:10.1016/j.expneurol.2014.04.024.

Decreased SIRT2 activity leads to altered microtubule dynamics in oxidatively-stressed neuronal cells: Implications for Parkinson's disease

Vivek P. Patel and **Charleen T. Chu***
Department of Pathology, Division of Neuropathology; University of Pittsburgh, Pittsburgh, PA, 15261, U.S.A.

Abstract

The microtubule (MT) system is important for many aspects of neuronal function, including motility, differentiation, and cargo trafficking. Parkinson's disease (PD) is associated with increased oxidative stress and alterations in the integrity of the axodendritic tree. To study dynamic mechanisms underlying the neurite shortening phenotype observed in many PD models, we employed the well-characterized oxidative parkinsonian neurotoxin, 6-hydroxydopamine (6OHDA). In both acute and chronic sub-lethal settings, 6OHDA-induced oxidative stress elicited significant alterations in MT dynamics, including reductions in MT growth rate, increased frequency of MT pauses/retractions, and increased levels of tubulin acetylation. Interestingly, 6OHDA decreased the activity of tubulin deacetylases, specifically sirtuin 2 (SIRT2), through more than one mechanism. Restoration of tubulin deacetylase function rescued the changes in MT dynamics and prevented neurite shortening in neurondifferentiated, 6OHDA-treated cells. These data indicate that impaired tubulin deacetylation contributes to altered MT dynamics in oxidatively-stressed cells, conferring key insights for potential therapeutic strategies to correct MT-related deficits contributing to neuronal aging and disease.

Keywords

Microtubule dynamics; oxidative stress; Parkinson's disease; sirtuin

*Charleen T. Chu (**Corresponding author**), 3550 Terrace St., Rm. S701 Scaife Hall, Pittsburgh, PA, 15261, U.S.A., Phone: 412-383-5379, Fax: 412-648-9527, ctc4@pitt.edu.
V. P. Patel, 3550 Terrace St., Rm. S782 Scaife Hall, Pittsburgh, PA, 15261, U.S.A. (vpp3@pitt.edu)

Author Contributions
VP and CC both contributed to the conception and design of the study, interpretation of the data, and preparation of the article. VP also collected and analyzed the data.

Conflicts of Interest
The authors declare that they have no actual or potential conflicts of interest related to the content of this paper.

Introduction

Neurodegenerative diseases, such as Parkinson's disease (PD), are associated with alterations in the integrity of the axon/dendrites, axonal transport of organelles, and gene expression in affected neurons (Burke and O'Malley, 2012; Courtney et al., 2010; Gunawardena and Goldstein, 2004; G. A. Morfini et al., 2009). A better understanding of the specific mechanisms that underlie such alterations is crucial for elucidating pathogenic mechanisms underlying PD and for the development of novel therapeutic strategies. The microtubule (MT) system may play an important role in PD pathogenesis. It is crucial for many aspects of neuronal function, including motility, differentiation, and protein and organelle trafficking (Conde and Caceres, 2009; De Vos et al., 2008; G. A. Morfini, et al., 2009). Hence, dysregulation of this system can have a significant impact on neuronal function, as well as explaining multiple cellular phenotypes observed in degenerating neurons in PD.

MTs are highly dynamic structures, continuously undergoing phases of growth (polymerization) and shrinkage (depolymerization) – a property known as dynamic instability (Cooper, 2000; Galjart, 2010). This property of MTs is crucial to its function and is regulated by a large network of proteins, MT-associated proteins (MAPs), that interact with one another in a complex manner (Akhmanova and Steinmetz, 2008; Cooper, 2000; Galjart, 2010; van der Vaart et al., 2009). Furthermore, MT function is also regulated by post-translational modifications (PTMs) of the tubulin subunit, such as acetylation, tyrosination / detyrosination, and polyglutamylation (Fukushima et al., 2009; Janke and Kneussel, 2010). These PTMs affect the binding of various MAPs and may even directly influence the stability of the MT structure (Fukushima, et al., 2009; Ikegami et al., 2007; Janke and Bulinski, 2011; Kubo et al., 2010). Despite increasing basic knowledge concerning the regulation of MT dynamics, relatively little is known of mechanisms that disrupt MT function in PD models.

Oxidative stress is thought to play a key role in the pathogenesis and/or progression of PD, particularly since degenerating brain regions often handle oxidative catecholaminergic neurotransmitters. Post-mortem human PD brains show significant oxidative damage to proteins, lipids, and DNA (Alam, Daniel, et al., 1997; Alam, Jenner, et al., 1997; Floor and Wetzel, 1998; Nakabeppu et al., 2007; Yoritaka et al., 1996). In addition, genetic (e.g. *PARK2* (Parkin), *PINK1* (PTEN-induced kinase 1), *SNCA* (α-synuclein), *DJ-1*, and *LRRK2* (leucine-rich repeat kinase 2)) and toxin (6-hydroxydopamine (6OHDA), 1-methyl-4-phenyl-1,2,3,6-tetrahydropyridine (MPTP), rotenone, and paraquat) models provide strong evidence for the involvement of oxidative stress in PD (Drechsel and Patel, 2008; Hisahara and Shimohama, 2010; Ross and Smith, 2007; Tan and Skipper, 2007; Terzioglu and Galter, 2008). Oxidative stress, which affects many cellular processes, could also alter MT dynamics and lead to significant defects in MT-dependent processes. A few studies in non-neuronal cell types indicate that acute, bolus treatments with high dose of hydrogen peroxide (H_2O_2) disrupt tubulin polymerization (C. F. Lee et al., 2005; Smyth et al., 2010). However, the effects of sub-lethal oxidative stress in neuronal cells have not been examined, although such conditions may be more pertinent for this chronic, degenerative disease. The goal of

this study was to examine the effects of sub-lethal oxidative stress, as induced by the PD toxin 6OHDA, on MT function in neuronal cells.

6OHDA has been widely used, *in vivo* and *in vitro*, to study neuronal injury responses in PD (Blum et al., 2001; Bove et al., 2005). After being taken up into cells by dopamine reuptake transporters, it generates reactive oxygen species (ROS) through several mechanisms that include redox-cycling autoxidation, oxidation by monoamine oxidases, and the secondary onset of mitochondrial dysfunction (Blum, et al., 2001; Kulich et al., 2007; Przedborski and Ischiropoulos, 2005). 6OHDA alters the subcellular localization of certain transcription factors (Dagda et al., 2008; V. P. Patel et al., 2012; Zhu et al., 2002), leading to alterations in gene transcription and decreased survival of midbrain neurons and catecholaminergic SH-SY5Y cells (Chalovich et al., 2006). These findings are consistent with changes observed in degenerating midbrain neurons of post-mortem PD brains (C. T. Chu et al., 2007). Moreover, 6OHDA affects the levels of polymerized tubulin, and selectively impairs the nuclear import of a MT-sensitive transcription factor (V. P. Patel, et al., 2012). In this study, we utilized both a pre-lethal and a sub-lethal 6OHDA injury paradigm to examine in detail the impact of oxidative stress on MT dynamics.

Materials and Methods

Tissue Culture

Human SH-SY5Y neuroblastoma cells (ATCC, Manassas, VA) were grown on 10cm cell culture dishes containing Dulbecco's Modified Eagle's Medium (DMEM) with 10% fetal calf serum (BioWhittaker, Walkersville, MD), 2mM L-glutamine (BioWhittaker, Walkersville, MD), and 10mM HEPES (BioWhittaker, Walkersville, MD). For retinoic acid (RA) differentiation (Sigma-Aldrich, St. Louis, MO), cells were plated in 10μM RA for 3 days prior to any experimental manipulations, such as transfections or drug treatments, and then maintained in RA-containing media for the duration of the experiment. Cells were maintained at 37°C in a humidified 5% CO_2 incubator.

Plasmids & Transfections

The following plasmids were used: eGFP-C1 (Clontech, Mountain View, CA), pcDNA 3.1 (Invitrogen, Grand Island, NY), EB3-GFP (Niels Galjart, Erasmus University, Rotterdam, The Netherlands), HDAC6-FLAG (Addgene, Cambridge, MA), HDAC6-GFP (Francisco Sanchez-Madrid, Hospital Universitario de la Princesa, Instituto de Investigación Sanitaria Princesa, Madrid, Spain), SIRT2-FLAG (Addgene, Cambridge, MA), and SIRT2-GFP (Eric Verdin, UCSF, San Francisco, CA). EB3-mCherry was produced via standard subcloning techniques. Briefly, EB3-GFP and mCherry-N1 (Clontech, Mountain View, CA) were cleaved with EcoRI (New England BioLabs, Ipswich, MA) and BamHI (New England BioLabs, Ipswich, MA) for 1hr at 37°C and the cleaved products were separated on a 2.5% agarose (Invitrogen, Carlsbad, CA) gel. The appropriate gel bands were excised and the extracted DNAs (QIAquick Gel Extraction Kit; QIAGEN, Valencia, CA) ligated overnight with the Fast-Link™ DNA Ligation Kit (Epicentre Biotechnologies, Madison, WI) as per the manufacturer's protocol. The sequence of the ligated product, EB3-mCherry, was

confirmed (Sequencing Core Facility, Genomics and Proteomics Core Laboratories, University of Pittsburgh, Pittsburgh, PA).

SH-SY5Y cells were transfected using the Lipofectamine™ 2000 reagent (Invitrogen, Carlsbad, CA) utilizing Opti-MEM® I reduced serum media (Invitrogen, Carlsbad, CA) according to the manufacturer's protocol at a final Lipofectamine concentration of 0.1%. Undifferentiated SH-SY5Y cells were cultured for at least 2 days before transfection and then allowed to express the protein of interest for another 48hr before treatment. Differentiated SH-SY5Y cells were cultured for 3 days before transfection and the treatments were initiated 24hr after transfection.

Pharmacological Treatments

Retinoic acid was prepared in dimethyl sulfoxide (DMSO) at a stock concentration of 10mM and stored at −20°C. 6OHDA (Sigma-Aldrich, St. Louis, MO) was prepared in cold sterile water immediately before each use. NAD+ (Sigma-Aldrich, St. Louis, MO) was dissolved in sterile water at a stock concentration of 50mM and stored at −80°C. Mn (III) tetrakis (4-benzoic acid) porphyrin (MnTBAP) (A.G. Scientific, San Diego, CA) was initially dissolved in 0.1M NaOH and then diluted in 100mM Hepes to make a 3mM stock solution. The pH of the solution was brought to 7.0 – 7.2 and then it was sterile filtered before storage at 4°C. All drugs were used at concentrations as indicated in the Results section and handled to minimize light exposure.

Cell Toxicity Assays

Lactate Dehydrogenase (LDH) Release Assay: Cells were plated in a black, clear-bottom 96-well plate and treated with 6OHDA for varying dosage and time. LDH release was measured using the CytoTox-ONE Homogeneous Membrane Integrity Assay per the protocol provided by the manufacturer (Promega, Madison, WI). Percent cytotoxicity was calculated by the following formula: 100 * [(Experimental – Medium Background) / (Maximum LDH release – Medium Background)]. Maximum LDH release was determined by treatment of cells with lysis buffer as per manufacturer's protocol.

MTS Assay—Cells were plated in a clear 96-well plate and treated with 6OHDA for varying dosage and time. Cell toxicity resulting from 6OHDA was determined via the CellTiter 96 Aqueous Non-Radioactive Cell Proliferation Assay (MTS) as per the manufacturer's protocol (Promega, Madison, WI). Since 6OHDA oxidation itself can cause media color changes, a parallel 96-well plate with only media was similarly treated with 6OHDA to establish background readings.

A Spectramax M2 plate reader (Molecular Devices, Sunnyvale, CA) was utilized to quantify the signals from these assays.

ROS Measurement

To measure ROS levels, SH-SY5Y cells treated with MnTBAP and/or 6OHDA were incubated in CellRox® Green reagent as per the protocol provided by the manufacturer (Life Technologies, Carlsbad, CA). This cell-permeable dye becomes highly fluorescent once it

becomes oxidized by ROS and then binds to DNA. Stained cells were placed in pre-warmed Dulbecco's Phosphate buffered Saline (DPBS) containing glucose (Life Technologies, Carlsbad, CA) and immediately imaged on an Olympus IX71 inverted microscope with a 40× oil objective. All images were acquired at an exposure time of 500ms. The integrated fluorescence intensity was measured using NIH ImageJ 1.46 (Bethesda, MD).

Immunocytochemistry

For EB1 protein detection, media was removed and the cells were immediately fixed in −20°C methanol (Fisher Scientific, Pittsburgh, PA) for 5min. For all other stains, cells were fixed in 4% paraformaldehyde (Sigma-Aldrich, St. Louis, MO) prepared in phosphate buffered saline (PBS) for 30min at room temperature. Cells were permeabilized with 0.1% Triton X-100 (Fisher Scientific, Pittsburgh, PA) in PBS for 20min and then blocked with a commercial blocking buffer (SuperBlock, Thermo Scientific, Rockford, IL) for 1hr at room. Cells were incubated in primary antibody overnight at 4°C or 1hr at room temperature. Secondary antibody was used at a dilution of 1:1000 for 1hr at room temperature. Both primary and secondary antibodies were diluted in a commercial antibody diluent (BioGenex, Fremont, CA). Primary antibodies used: α-tubulin (1:5000; Sigma-Aldrich, St. Louis, MO), acetylated-tubulin (1:1000; Sigma-Aldrich, St. Louis, MO), EB1 (1:500; BD Biosciences, San Jose, CA), FLAG (1:5000; Sigma-Aldrich, St. Louis, MO), HDAC6 (1:1000; Santa Cruz Biotechnology, Santa Cruz, CA), and SIRT2 (1:1000; Sigma-Aldrich, St. Louis, MO). Secondary antibodies used: Alexa Fluor-488 (Invitrogen, Carlsbad, CA) and Cy3 (Jackson ImmunoResearch Laboratories, West Grove, PA).

Immunoblotting

Immunoblots were performed as previously described (V. P. Patel, et al., 2012; Zhu et al., 2007). Primary antibodies used: acetylated tubulin (1:10:000; Sigma-Aldrich, St. Louis, MO), α-tubulin (1:5:000; Sigma-Aldrich, St. Louis, MO), GAPDH (1:10:000; Abcam, Cambridge, MA), HDAC6 (1:5000; Santa Cruz Biotechnology, Santa Cruz, CA), and SIRT2 (1:500; Sigma-Aldrich, St. Louis, MO). ImageJ was utilized for densitometry.

Immunoprecipitation & Deacetylase Activity Assay

Cells were lysed in lysis buffer (50mM Tris HCl pH 8.0, 137mM NaCl, 2.5mM EDTA pH 8.0, 1% Triton X-100, 1mM sodium orthovanadate, and 1:100 dilution of protease inhibitor cocktail (Sigma-Aldrich, St. Louis, MO)) for at least 30min at 4°C with constant agitation. Lysates were centrifuged at 14,000 × *g* for 15min. The protein concentration of the supernatant was determined using the Coomassie Plus (Bradford) protein assay (Thermo Scientific, Rockford, IL). One mg of protein was added to 50μL of Protein A-Agarose beads (Sigma-Aldrich, St. Louis, MO) that had been previously washed 5 times in 500μL lysis buffer. Two μg of HDAC6, 3μg of SIRT2, or equivalent amounts of IgG (Vector Laboratories, Burlingame, CA) were added to the lysate/bead mixture and incubated overnight at 4°C with constant agitation. The beads were collected by centrifugation at 0.1 ×*g* for 5min, washed 3 times in lysis buffer with protease inhibitors, and washed twice in HDAC Assay Buffer (Enzo Life Sciences, Farmingdale, NY).

The activity of the pulled-down deacetylase was measured using the Fluor-de-Lys-Green HDAC fluorometric activity assay kit (Enzo Life Sciences, Farmingdale, NY) as per the manufacturer's protocol. Briefly, 100μM Fluor-de-Lys-Green substrate that contains an acetylated lysine side chain was added to the bead/antibody/enzyme mixture and the reaction was carried out for 15min to 1hr at 37°C with constant agitation. For SIRT2 activity, 500μM NAD+ was also added to the reaction. Once the reaction was complete, 50μL of the reaction solution was added to an opaque, white, ½-volume 96-well plate and 50μL of a Fluor-de-Lys Developer solution containing 2μM Trichostatin A (for HDAC6 inhibition; final concentration 1μM) or 2μM nicotinamide (for SIRT2 inhibition; final concentration 1μM) was added. The plate was incubated at room temperature for at least 20min and the fluorescent signal was read (excitation: 485nm; emission: 530nm) using a Spectramax M2 plate reader.

NAD+ / NADH Quantification

A NAD+/NADH Quantitation Kit was utilized as per the manufacturer's protocol (BioVision, Milpitas, CA). Briefly, cells were washed in DPBS, trypsinized (BioWhittaker, Walkersville, MD), and collected in media. 2 million cells were pelleted at 1000 × *g* for 5min and the pellet was washed twice with DPBS. 400μL of Extraction Buffer was added and two freeze/thaw cycles (20min on dry-ice and 15min at room temperature) were carried out to extract NAD+ and NADH. After vortexing and centrifugation, some of the sample was saved for a protein assay. The remaining sample was filtered through a 10kD molecular weight cut off filter (Abcam, Cambridge, MA) to remove any enzymes that could consume NAD+ or NADH. Absorbance was read at 450nm using a Spectramax M2 plate reader. A BCA (bicinchoninic acid) protein assay (Thermo Scientific, Rockford, IL) was carried out on a portion of each sample and NAD+ / NADH absorbance values were normalized to protein concentration.

Live-Cell Imaging of MT Dynamics

To study MT dynamics, cells expressing fluorescently-tagged EB3 were transferred in pre-warmed DPBS containing glucose to an Olympus IX71 inverted microscope with a 60× oil objective and a heated stage set to 37°C (Warner Instruments, Hamden, CT). Analysis was restricted to cells exhibiting low-level expression of EB3-GFP / EB3-mCherry that allowed resolution of a clear comet-like pattern, as it has been shown that low-level expression of such proteins does not affect the dynamic behavior of MTs (Stepanova et al., 2003). Images were taken every 5sec at an exposure time of 500ms (EB3-GFP) or 1sec (EB3-mCherry). A neutral density filter that reduces light intensity by 50% was used for all live cell imaging to minimize ultraviolet light exposure.

Neurite Length Measurement & Image Analysis

Neurite length was measured in GFP expressing cells using NIH ImageJ 1.46. At least 50 neurites were quantified for each group of each independent experiment. EB comet length was measured in cells that were imaged at the same exposure time and, using ImageJ, thresholded with the same parameters to minimize the background noise and to highlight the EB comets. The longest distance between two points (Feret's diameter) was determined for

each comet. At least 10 comets per cell and at least 5 cells were analyzed for each group of each independent experiment. For MT growth rate measurements, EB3 comets that could be followed for at least three consecutive frames were measured using the MTrackJ plugin for ImageJ (Meijering et al., 2012). For measurements of pauses/retractions, the number of comet dimming events, time elapsed in each dimming event, and time between two dimming events was determined. For measurements of growth rate and pauses/retractions, at least 5 comets per cell and at least 5 cells were analyzed for each group of each independent experiment. All data was derived from at least three independent experiments.

Statistical Analysis

Student's *t* test was used for comparison of means between two groups. One-way analysis of variance (ANOVA) followed by post-hoc Tukey HSD test was used for multiple comparisons. A p-value < 0.05 was considered statistically significant.

Results

6OHDA-induced oxidative stress alters MT dynamics

Our previous study showed that a short-term exposure to 6OHDA-induced oxidative stress leads to an early impairment in MT-dependent transcription factor trafficking in SH-SY5Y cells, a dopaminergic neuronal cell line used to model PD mechanisms (Lopes et al., 2010; V. P. Patel, et al., 2012; Xie et al., 2010). Such pre-lethal treatments with 6OHDA do not cause significant cellular toxicity (Supplementary Fig. S1). The effects of 6OHDA-induced oxidative stress on MT dynamics were examined using a fluorescently-tagged end-binding protein 3 (EB3), which belongs to the family of plus-end tracking proteins (+TIPs) that bind to MT growing (plus) ends (Akhmanova and Steinmetz, 2008; Galjart, 2010; van der Vaart, et al., 2009). Fluorescently-tagged +TIPs, such as EBs, have been extensively characterized for the study of MT dynamics in living cells (Chan et al., 2003; Matov et al., 2010; Stepanova, et al., 2003). SH-SY5Y cells expressing EB3-GFP were treated with a pre-lethal dose of 6OHDA (150μM; 4hrs) and the MT growth rate was determined. Fig. 1A shows an example of EB3-GFP comet movement with time, which was quantified to determine the MT growth rate. A significant reduction in MT growth rate was observed in 6OHDA-treated cells (Fig. 1B). Videos 1–3 provide examples of MT dynamics in control (Video 1) and 6OHDA-treated cells (Video 2 and 3). The length of the EB comets is positively correlated with MT growth rate (Bieling et al., 2008; Matov, et al., 2010; Tirnauer et al., 2002). Thus, the comet lengths of endogenous EBs can also be used as a measure of MT growth rates. With pre-lethal 6OHDA injury, cells showed decreased endogenous EB1 comet length, which suggests reduced growth rates as consistent with the live cell data (Fig. 1C & D).

In addition to the pre-lethal injury paradigm, we also developed a sub-lethal treatment protocol to investigate the effects of more prolonged oxidative stress, which is relevant to studies of aging and neurodegenerative diseases. For these studies, examining neurite integrity was of particular interest since axonopathy may represent an early change in PD (Burke and O'Malley, 2012). SH-SY5Y cells were differentiated with retinoic acid to a more mature neuronal phenotype, biochemically as well as morphologically (Encinas et al., 2000; Lopes, et al., 2010; Xie, et al., 2010). Viability assays with varying concentrations of

6OHDA showed that concentrations ≤ 30μM did not cause cell death (Supplementary Fig. S2). Hence, for studying the effects of sub-lethal oxidative stress on MT dynamics, differentiated cell were treated with 30μM 6OHDA every 24hr for a total of 72hr (3 total treatments) and MT dynamics along the length of the neurite was examined (24hr after the last treatment).

Sub-lethal 6OHDA treatment also caused a reduction in MT growth rates, albeit to a lesser extent (Fig. 2A). Moreover, the regular alignment of MTs in the neurites facilitated assessments of additional parameters of MT dynamics in the sub-lethal model. EBs, along with other +TIPs, only bind to the MTs when they are growing (Akhmanova and Steinmetz, 2008; Galjart, 2010). Therefore, during pauses or retractions, the MT ends dim when using fluorescently-tagged EB3 to visualize them, as shown in Figure 2B. If the MT in this example had paused for a longer period of time, all of the EB3-GFP at the MT plus-end would have been lost and the MT would no longer be visible. As the MT beings to grow again, the fluorescent intensity of the EB3-GFP comet is again increased. Given this feature of +TIPs, one can study other important aspects of MT dynamics besides growth rate, such as frequency and length of MT pauses/retractions. Since it is sometimes difficult to differentiate between a pause and a retraction, each “dimming” event will be referred to as a pause and/or retraction event, or a “P/R” event. Sub-lethal 6OHDA treatment increased the frequency of the P/R events (Fig. 2C) and caused individual MTs to pause/retract more frequently over a given period of time. These resulted in a lower percentage of MTs exhibiting 0 to 1 P/R events and a greater percentage exhibiting 2 or more P/R events (Fig. 2D). The amount of time that elapsed between two P/R events was reduced; however the duration of an individual P/R event was not altered (Fig. 2E & 2F). In short, significant alterations in several aspects of MT dynamics, including MT growth rate and frequency of pauses/retractions, are observed in cells subjected to sub-lethal oxidative stress.

The effects of sub-lethal 6OHDA injury on EB1 along the length of the neurite was also examined (Fig. 3). Compared to undifferentiated cell bodies, a more punctate pattern of EB1 fluorescence is observed along the neurite in differentiated control cells, making static comet length analysis less meaningful (Fig. 3A). However, the levels of EB1 can be accurately assessed, which may also provide valuable information about MT dynamics (Coquelle et al., 2009). Indeed, sub-lethal 6OHDA decreased EB1 staining along the length of the neurite (Fig. 3A) and this reduction was confirmed by Western blot analysis of total cellular EB1 content (Fig. 3B).

As expected, both pre-lethal and sub-lethal 6OHDA increased ROS levels in SH-SY5Y cells (Fig. 4A & 4B). Pre-treatment with Mn (III) tetrakis (4-benzoic acid) porphyrin (MnTBAP), a metalloporphyrin antioxidant that possesses superoxide dismutase and catalase-like activities (Day et al., 1997; M. Patel and Day, 1999), significantly reduced ROS levels in 6OHDA-treated cells (Fig. 4A & 4B). Cells were treated with 200μM MnTBAP 30min prior to pre-lethal 6OHDA injury or 30μM MnTBAP 30min prior to sub-lethal 6OHDA injury. We then studied the effects of antioxidant pre-treatment on MT dynamics. MnTBAP pre-treatment rescued the impairment of MT growth rate after pre-lethal 6OHDA injury (Fig. 4C). The increase in the frequency of MT pauses / retractions after sub-lethal 6OHDA injury was also significantly reduced in MnTBAP pre-treated cells (Fig. 4D). Hence, 6OHDA

causes significant alterations in MT dynamics through the generation of ROS in both models.

To summarize, both the live cell and static methods of analyses show that the oxidative neurotoxin 6OHDA causes significant alterations in MT dynamics that could contribute to PD-related changes in axonal integrity and protein or organelle transport.

6OHDA increases tubulin acetylation by impairing tubulin deacetylase function

To examine potential underlying mechanisms by which 6OHDA regulated MT dynamics, we examined tubulin acetylation, which serves to regulate MT dynamics through numerous mechanisms (Choudhary et al., 2009; Fukushima, et al., 2009; Janke and Bulinski, 2011; Sudo and Baas, 2010; Tran et al., 2007). Similar to effects described for the PD toxin MPP+ (Cartelli et al., 2010), we found that both pre-lethal and sub-lethal doses of 6OHDA lead to a significant increase in the level of tubulin acetylation (Fig. 5A & 5B).

We next examined the mechanism(s) by which 6OHDA may cause an increase in tubulin acetylation. Two major tubulin deacetylases are histone deacetylase 6 (HDAC6) and sirtuin 2 (SIRT2). Interestingly, H_2O_2 and cigarette smoke have been linked to altered localization, levels, and/or activity of various other HDACs, e.g. HDAC1, HDAC2, HDAC4, and SIRT1, in a variety of models (Ago et al., 2008; Doyle and Fitzpatrick, 2010; Ito et al., 2004; S. R. Yang et al., 2006; Y. Yang et al., 2007). Given the structural similarities of the deacetylase domain between the various classes of HDACs, we hypothesized that HDAC6 and/or SIRT2 may also be sensitive to oxidative stress and hence examined the effects of 6OHDA on their subcellular localization, protein levels, and enzymatic activity. HDAC6 and SIRT2 are predominantly cytoplasmic proteins that may also localize to the nucleus under certain conditions (North et al., 2003; North and Verdin, 2007; Verdel et al., 2000). The subcellular localization of HDAC6 and SIRT2 was not altered in response to pre-lethal or sub-lethal 6OHDA treatment (Supplementary Fig. S3). Protein levels of HDAC6 and SIRT2 were also not significantly altered after pre-lethal or sub-lethal 6OHDA treatment (Supplementary Fig. S4). To determine enzymatic activity, cells were treated with either pre-lethal or sub-lethal 6OHDA and endogenous HDAC6 or SIRT2 was immunoprecipitated. No significant change in the activity of HDAC6 was observed in either of the 6OHDA injury paradigms (Fig. 6A & 6B). Likewise the activity of immunoprecipitated SIRT2 was not changed after 4hr in the pre-lethal model (Fig. 6C). However, sub-lethal 6OHDA treatments over 72hr led to a reduction in SIRT2 activity (Fig. 6D).

To further investigate potential mechanisms underlying the increases in tubulin acetylation, we investigated the status of NAD+ and NADH within 6OHDA-stressed cells. NAD+ is an essential co-factor for SIRT2 deacetylase activity and is an important determinant of the redox state of the cell (Furukawa et al., 2007; Michan and Sinclair, 2007). A reduction in NAD+ levels after acute pre-lethal 6OHDA exposure could lead to reduced SIRT2 activity within cells, even if immunoprecipitated SIRT2 can still function normally in the presence of added co-factor. Using an enzyme cycling reaction, the levels of NAD+ and NADH were examined in cells treated with either pre-lethal or sub-lethal 6OHDA. A significant reduction in both NAD+ and NADH was observed after pre-lethal 6OHDA exposure but not sub-lethal 6OHDA exposure (Fig. 7). The combined results suggest that different

mechanisms are involved in the altered levels of tubulin acetylation that is observed. After 4hr of higher dose pre-lethal injury, significant reduction in levels of the co-factor NAD+ leads to diminished SIRT2 function in cells. However, after 72hr of lower dose sub-lethal injury, there is a significant reduction in the intrinsic enzymatic activity of SIRT2. The end results of these changes are the same – an increase in the levels of tubulin acetylation that may contribute to the impaired MT growth kinetics observed in both models.

Restoring deacetylase function rescues the impairment in MT dynamics

Next, we examined if restoring tubulin deacetylase function in cells could rescue the MT phenotype elicited by 6OHDA. First, given the reduction in NAD+ levels in the pre-lethal injury model, the effects of restoring cellular NAD+ levels on MT dynamics in the pre-lethal model was examined. The addition of NAD+ to the culture medium can effectively increase intracellular NAD+ levels in a variety of cell lines, including SH-SY5Y cells (Billington et al., 2008; Caito, Hwang, et al., 2010; Pittelli et al., 2011). Indeed, we found that the addition of NAD+ (1mM) for 6hr to the culture medium caused an increase in the levels of intracellular NAD+ (Fig. 8A). To examine the effects of NAD+ restoration on 6OHDA-mediated increase in tubulin acetylation levels, cells were treated with vehicle or NAD+ for 6hrs before treatment with pre-lethal 6OHDA (added directly to the medium containing NAD+). The 6OHDA-mediated increase in tubulin acetylation was significantly reduced in cells that were pre-treated with NAD+ (Fig. 8B & 8C). To study the effects of NAD+ restoration on MT growth rate, cells expressing fluorescently-tagged EB3 were treated with NAD+ and pre-lethal 6OHDA as mentioned above. In cells that were pre-treated with NAD +, a rescue in MT growth rate was observed (Fig. 8D). These results suggest that restoration of NAD+ levels and hence SIRT2 function reverses the changes in tubulin acetylation and MT dynamics in 6OHDA-treated cells.

The effect of directly increasing the expression of the tubulin deacetylases was also examined. GFP, HDAC6-GFP, or SIRT2-GFP was transfected along with EB3-mCherry into SH-SY5Y cells and MT dynamics was examined via live cell imaging as before. First, the effect on MT growth rate was examined in the pre-lethal model. Overexpression of either HDAC6-GFP or SIRT2-GFP resulted in a reduction in the impairment of MT growth rate from 6OHDA-induced oxidative stress (Fig. 9A). For sub-lethal injury, the most significant alteration in MT dynamics was an increase in frequency of pauses / retractions. This effect was confirmed in cells expressing just GFP (Fig. 9B). However, a significant rescue was observed in cells expressing either HDAC6-GFP or SIRT2-GFP (Fig. 9B). Therefore, the overexpression of either HDAC6 or SIRT2 protects against 6OHDA-induced alteration in MT dynamics.

Restoring deacetylase function rescues against 6OHDA-mediated neurite shortening

MTs play a key role in the development and maintenance of neuritic processes (axons and dendrites). Indeed, exposure of neuron-differentiated SH-SY5Y cells to sub-lethal oxidative stress reduced the length of their neurites (Fig. 10A & 10B). Given that modulation of tubulin deacetylases affects MT dynamics, we examined whether or not rescue of MT dynamics can also rescue neurite integrity. Cells were transfected with pcDNA, HDAC6-FLAG, or SIRT2-FLAG and then treated with sub-lethal 6OHDA. Control cells expressing

SIRT2-FLAG showed slightly reduced neurite lengths compared to pcDNA control (data not shown), as consistent with the literature (Pandithage et al., 2008). Nonetheless, the percent reduction in neurite length in response to 6OHDA-induced oxidative stress was significantly lower in cells expressing either HDAC6-FLAG or SIRT2-FLAG compared to pcDNA control (Fig. 10B).

Discussion

In this study, we found that the oxidative neurotoxin 6OHDA has a significant impact on neuronal MT function through modulation of SIRT2 function. These alterations in MT function were observed both early in acute injuries and in the context of chronic, sub-lethal injury in neuron-differentiated SH-SY5Y cells, the latter of which may have particular relevance to PD mechanisms (Lopes, et al., 2010; Xie, et al., 2010).

The altered levels of acetylated tubulin resulted from the impaired function of the tubulin deacetylase SIRT2; however, the underlying mechanisms differed between the two models. Pre-lethal but not sub-lethal 6OHDA exposure caused a significant decline in intracellular NAD+ and NADH levels, contributing to cellular SIRT2 dysfunction through depletion of its essential co-factor. One possible mechanism reflects overconsumption of NAD+ in acutely stressed cells. NAD+ is consumed by numerous enzymes, including the poly(ADP-ribose) polymerases-1 (PARP-1), which senses DNA damage (Pittelli, et al., 2011; Rouleau et al., 2010; Virag and Szabo, 2002; Ying, 2008). Reactive oxygen species such as H_2O_2 and hydroxyl radical cause significant DNA strand breakage, which results in over-activation of PARP-1 followed by depletion of NAD+ and subsequently ATP (Virag and Szabo, 2002). This process is thought to play a key pathogenic role in stroke, diabetes, myocardial ischemia, hemorrhagic and septic shock, various forms of inflammation, traumatic brain injury, and MPTP-induced parkinsonism (Mandir et al., 1999; Virag and Szabo, 2002). Furthermore, oxidative stress can shift the balance of reduced pyridine nucleotides away from NADH and towards NADPH, which helps in the defense against ROS, by the regulation of various NADPH and NADH forming dehydrogenases and NAD kinases (Grose et al., 2006; Jo et al., 2001; Pollak et al., 2007; Singh et al., 2007; Ursini et al., 1997; Vasiliou and Nebert, 2005). The end result involves impairment in NAD+ dependent activities including SIRT2-mediated deacetylation.

Depletion of NAD+ cofactors specifically in the higher dose pre-lethal model may reflect significantly higher degree of ROS generated in the pre-lethal model – leading to greater consumption of NAD+ and reduced regeneration from NADH by the mechanisms mentioned above. It is also possible that there is a transient dip in NAD+ / NADH levels after each administration of the sub-lethal dose that recovers by the time measurements are taken 24hr after the final dose. Nonetheless, after 3 days of sub-lethal oxidative stress, a decline in the intrinsic deacetylase activity of immunoprecipitated SIRT2 was observed. As total levels of SIRT2 are unchanged between control cells and 6OHDA-stressed cells (Supplementary Fig. S4), it is possible that post-translational modifications are involved. Carbonylation, cysteine oxidation, and S-glutathiolation have each been reported to regulate SIRT1 function and there is conservation of the primary structure of the catalytic domains between SIRT1 and SIRT2 (Caito, Rajendrasozhan, et al., 2010; Michan and Sinclair, 2007;

Zee et al., 2010). Future studies to delineate post-translational modifications of SIRT2 under conditions of low-level, chronic oxidative stress may yield valuable insights for PD pathogenesis.

Tubulin acetylation may play an important role in regulating MT function (Choudhary, et al., 2009; Fukushima, et al., 2009; Janke and Bulinski, 2011; Sudo and Baas, 2010; Tran, et al., 2007). In this study, overexpression of either HDAC6 or SIRT2 reversed the changes in MT dynamics observed in both models, suggesting that increased tubulin acetylation is most likely responsible for a significant portion of the alteration in MT dynamics. In the pre-lethal injury model, overexpression of SIRT2 was able to rescue MT function similar to HDAC6 despite reduced NAD+ levels. As SIRT2 competes with numerous other enzymes for NAD +, its overexpression may allow it to compete more effectively for available NAD+, leading to an overall increase in tubulin deacetylase activity.

The mechanism by which tubulin acetylation regulates MT biology is not clear in the literature. However, possible mechanisms include conformational changes, altered sensitivity to MT lattice severing by katanin, or impaired incorporation into growing MTs (C. W. Chu et al., 2011; Janke and Bulinski, 2011; Sudo and Baas, 2010). Indeed, either acetylation or oxidative modification (Landino et al., 2011; Luduena and Roach, 1991; Mellon and Rebhun, 1976) of the tubulin heterodimer impairs MT polymerization, consistent with the observation that pre-lethal doses of 6OHDA increase levels of monomeric tubulin (V. P. Patel, et al., 2012). Acetylation sites that are predicted to face the outside surface of the MT lattice could also serve to regulate MT dynamics by affecting the binding of MAPs, such as EBs (Choudhary, et al., 2009; Janke and Bulinski, 2011).

Conclusions

MTs are essential for the development and maintenance of axons and transport of cargo, such as organelle and protein complexes (Conde and Caceres, 2009; De Vos, et al., 2008; G. A. Morfini, et al., 2009). Various genetic as well as toxin models of PD suggest that MT dysfunction may be an important component of disease pathogenesis and/or progression. Genetic (α-synuclein, LRRK2, and PINK1) and other toxin (MPP+ and rotenone) models also exhibit alterations in axonal transport (Borland et al., 2008; Cartelli, et al., 2010; Chung et al., 2009; Kim-Han et al., 2011; H. J. Lee et al., 2006; Liu et al., 2012; G. Morfini et al., 2007; Pham et al., 2004; Saha et al., 2004). In this study, we show that 6OHDA-induced oxidative stress affects MT dynamics and SIRT2 activity through more than one mechanism, leading to neurite shortening, an important early phenotype in PD models. In addition to its impact on the integrity of the axon/dendrites and intracellular transport, disruption of MT function could also affect gene expression, leading to selective declines in the reparative transcriptional responses of diseased dopaminergic neurons (V. P. Patel, et al., 2012). In conclusion, MT dysfunction represents a point of convergence among different models of PD, suggesting an important role in the pathogenesis of PD. Elucidating how redox changes in MT function can lead to neuronal degeneration may provide key insights into the development of novel disease-modifying strategies.

Supplementary Material

Refer to Web version on PubMed Central for supplementary material.

Acknowledgments

Funding

This work was supported by the National Institute of Health [R01 AG026389 and R01 NS065789]. VP was supported in part by the National Institutes of Health [T32-NS007433 and F31-NS076040].

References

Ago T, Liu T, Zhai P, et al. A redox-dependent pathway for regulating class II HDACs and cardiac hypertrophy. Cell. 2008; 133:978–993. [PubMed: 18555775]

Akhmanova A, Steinmetz MO. Tracking the ends: a dynamic protein network controls the fate of microtubule tips. Nature reviews. Molecular cell biology. 2008; 9:309–322.

Alam ZI, Daniel SE, Lees AJ, Marsden DC, Jenner P, Halliwell B. A generalised increase in protein carbonyls in the brain in Parkinson's but not incidental Lewy body disease. Journal of neurochemistry. 1997; 69:1326–1329. [PubMed: 9282961]

Alam ZI, Jenner A, Daniel SE, et al. Oxidative DNA damage in the parkinsonian brain: an apparent selective increase in 8-hydroxyguanine levels in substantia nigra. Journal of neurochemistry. 1997; 69:1196–1203. [PubMed: 9282943]

Bieling P, Kandels-Lewis S, Telley IA, van Dijk J, Janke C, Surrey T. CLIP-170 tracks growing microtubule ends by dynamically recognizing composite EB1/tubulin-binding sites. The Journal of cell biology. 2008; 183:1223–1233. [PubMed: 19103809]

Billington RA, Travelli C, Ercolano E, et al. Characterization of NAD uptake in mammalian cells. The Journal of biological chemistry. 2008; 283:6367–6374. [PubMed: 18180302]

Blum D, Torch S, Lambeng N, et al. Molecular pathways involved in the neurotoxicity of 6-OHDA, dopamine and MPTP: contribution to the apoptotic theory in Parkinson's disease. Progress in neurobiology. 2001; 65:135–172. [PubMed: 11403877]

Borland MK, Trimmer PA, Rubinstein JD, et al. Chronic, low-dose rotenone reproduces Lewy neurites found in early stages of Parkinson's disease, reduces mitochondrial movement and slowly kills differentiated SH-SY5Y neural cells. Molecular neurodegeneration. 2008; 3:21. [PubMed: 19114014]

Bove J, Prou D, Perier C, Przedborski S. Toxin-induced models of Parkinson's disease. NeuroRx : the journal of the American Society for Experimental NeuroTherapeutics. 2005; 2:484–494. [PubMed: 16389312]

Burke RE, O'Malley K. Axon degeneration in Parkinson's disease. Experimental neurology. 2012

Caito S, Hwang JW, Chung S, Yao H, Sundar IK, Rahman I. PARP-1 inhibition does not restore oxidant-mediated reduction in SIRT1 activity. Biochemical and biophysical research communications. 2010; 392:264–270. [PubMed: 20060806]

Caito S, Rajendrasozhan S, Cook S, et al. SIRT1 is a redox-sensitive deacetylase that is post-translationally modified by oxidants and carbonyl stress. FASEB journal : official publication of the Federation of American Societies for Experimental Biology. 2010; 24:3145–3159. [PubMed: 20385619]

Cartelli D, Ronchi C, Maggioni MG, Rodighiero S, Giavini E, Cappelletti G. Microtubule dysfunction precedes transport impairment and mitochondria damage in MPP+ -induced neurodegeneration. Journal of neurochemistry. 2010; 115:247–258. [PubMed: 20649848]

Chalovich EM, Zhu JH, Caltagarone J, Bowser R, Chu CT. Functional repression of cAMP response element in 6-hydroxydopamine-treated neuronal cells. The Journal of biological chemistry. 2006; 281:17870–17881. [PubMed: 16621793]

Chan J, Calder GM, Doonan JH, Lloyd CW. EB1 reveals mobile microtubule nucleation sites in Arabidopsis. Nature cell biology. 2003; 5:967–971.

Choudhary C, Kumar C, Gnad F, et al. Lysine acetylation targets protein complexes and co-regulates major cellular functions. Science. 2009; 325:834–840. [PubMed: 19608861]

Chu CT, Plowey ED, Wang Y, Patel V, Jordan-Sciutto KL. Location, location, location: altered transcription factor trafficking in neurodegeneration. Journal of neuropathology and experimental neurology. 2007; 66:873–883. [PubMed: 17917581]

Chu CW, Hou F, Zhang J, et al. A novel acetylation of beta-tubulin by San modulates microtubule polymerization via down-regulating tubulin incorporation. Molecular biology of the cell. 2011; 22:448–456. [PubMed: 21177827]

Chung CY, Koprich JB, Siddiqi H, Isacson O. Dynamic changes in presynaptic and axonal transport proteins combined with striatal neuroinflammation precede dopaminergic neuronal loss in a rat model of AAV alpha-synucleinopathy. The Journal of neuroscience : the official journal of the Society for Neuroscience. 2009; 29:3365–3373. [PubMed: 19295143]

Conde C, Caceres A. Microtubule assembly, organization and dynamics in axons and dendrites. Nature reviews. Neuroscience. 2009; 10:319–332. [PubMed: 19377501]

Cooper, GM. Microtubules. The Cell: A Molecular Approach. 2nd edition. Sunderland, MA: Sinauer Associates; 2000.

Coquelle FM, Vitre B, Arnal I. Structural basis of EB1 effects on microtubule dynamics. Biochemical Society transactions. 2009; 37:997–1001. [PubMed: 19754439]

Courtney E, Kornfeld S, Janitz K, Janitz M. Transcriptome profiling in neurodegenerative disease. Journal of neuroscience methods. 2010; 193:189–202. [PubMed: 20800617]

Dagda RK, Zhu J, Kulich SM, Chu CT. Mitochondrially localized ERK2 regulates mitophagy and autophagic cell stress: implications for Parkinson's disease. Autophagy. 2008; 4:770–782. [PubMed: 18594198]

Day BJ, Fridovich I, Crapo JD. Manganic porphyrins possess catalase activity and protect endothelial cells against hydrogen peroxide-mediated injury. Archives of biochemistry and biophysics. 1997; 347:256–262. [PubMed: 9367533]

De Vos KJ, Grierson AJ, Ackerley S, Miller CC. Role of axonal transport in neurodegenerative diseases. Annual review of neuroscience. 2008; 31:151–173.

Doyle K, Fitzpatrick FA. Redox signaling, alkylation (carbonylation) of conserved cysteines inactivates class I histone deacetylases 1, 2, and 3 and antagonizes their transcriptional repressor function. The Journal of biological chemistry. 2010; 285:17417–17424. [PubMed: 20385560]

Drechsel DA, Patel M. Role of reactive oxygen species in the neurotoxicity of environmental agents implicated in Parkinson's disease. Free radical biology & medicine. 2008; 44:1873–1886. [PubMed: 18342017]

Encinas M, Iglesias M, Liu Y, et al. Sequential treatment of SH-SY5Y cells with retinoic acid and brain-derived neurotrophic factor gives rise to fully differentiated, neurotrophic factor-dependent, human neuron-like cells. Journal of neurochemistry. 2000; 75:991–1003. [PubMed: 10936180]

Floor E, Wetzel MG. Increased protein oxidation in human substantia nigra pars compacta in comparison with basal ganglia and prefrontal cortex measured with an improved dinitrophenylhydrazine assay. Journal of neurochemistry. 1998; 70:268–275. [PubMed: 9422371]

Fukushima N, Furuta D, Hidaka Y, Moriyama R, Tsujiuchi T. Post-translational modifications of tubulin in the nervous system. Journal of neurochemistry. 2009; 109:683–693. [PubMed: 19250341]

Furukawa A, Tada-Oikawa S, Kawanishi S, Oikawa S. H2O2 accelerates cellular senescence by accumulation of acetylated p53 via decrease in the function of SIRT1 by NAD+ depletion. Cellular physiology and biochemistry : international journal of experimental cellular physiology, biochemistry, and pharmacology. 2007; 20:45–54.

Galjart N. Plus-end-tracking proteins and their interactions at microtubule ends. Current biology : CB. 2010; 20:R528–R537. [PubMed: 20620909]

Grose JH, Joss L, Velick SF, Roth JR. Evidence that feedback inhibition of NAD kinase controls responses to oxidative stress. Proceedings of the National Academy of Sciences of the United States of America. 2006; 103:7601–7606. [PubMed: 16682646]

Gunawardena S, Goldstein LS. Cargo-carrying motor vehicles on the neuronal highway: transport pathways and neurodegenerative disease. Journal of neurobiology. 2004; 58:258–271. [PubMed: 14704957]

Hisahara S, Shimohama S. Toxin-induced and genetic animal models of Parkinson's disease. Parkinson's disease. 2010; 2011:951709.

Ikegami K, Heier RL, Taruishi M, et al. Loss of alpha-tubulin polyglutamylation in ROSA22 mice is associated with abnormal targeting of KIF1A and modulated synaptic function. Proceedings of the National Academy of Sciences of the United States of America. 2007; 104:3213–3218. [PubMed: 17360631]

Ito K, Hanazawa T, Tomita K, Barnes PJ, Adcock IM. Oxidative stress reduces histone deacetylase 2 activity and enhances IL-8 gene expression: role of tyrosine nitration. Biochemical and biophysical research communications. 2004; 315:240–245. [PubMed: 15013452]

Janke C, Bulinski JC. Post-translational regulation of the microtubule cytoskeleton: mechanisms and functions. Nature reviews. Molecular cell biology. 2011; 12:773–786. [PubMed: 22086369]

Janke C, Kneussel M. Tubulin post-translational modifications: encoding functions on the neuronal microtubule cytoskeleton. Trends in neurosciences. 2010; 33:362–372. [PubMed: 20541813]

Jo SH, Son MK, Koh HJ, et al. Control of mitochondrial redox balance and cellular defense against oxidative damage by mitochondrial NADP+-dependent isocitrate dehydrogenase. The Journal of biological chemistry. 2001; 276:16168–16176. [PubMed: 11278619]

Kim-Han JS, Antenor-Dorsey JA, O'Malley KL. The Parkinsonian mimetic, MPP+, specifically impairs mitochondrial transport in dopamine axons. The Journal of neuroscience : the official journal of the Society for Neuroscience. 2011; 31:7212–7221. [PubMed: 21562285]

Kubo T, Yanagisawa HA, Yagi T, Hirono M, Kamiya R. Tubulin polyglutamylation regulates axonemal motility by modulating activities of inner-arm dyneins. Current biology : CB. 2010; 20:441–445. [PubMed: 20188560]

Kulich SM, Horbinski C, Patel M, Chu CT. 6-Hydroxydopamine induces mitochondrial ERK activation. Free radical biology & medicine. 2007; 43:372–383. [PubMed: 17602953]

Landino LM, Hagedorn TD, Kim SB, Hogan KM. Inhibition of tubulin polymerization by hypochlorous acid and chloramines. Free radical biology & medicine. 2011; 50:1000–1008. [PubMed: 21256958]

Lee CF, Liu CY, Hsieh RH, Wei YH. Oxidative stress-induced depolymerization of microtubules and alteration of mitochondrial mass in human cells. Annals of the New York Academy of Sciences. 2005; 1042:246–254. [PubMed: 15965069]

Lee HJ, Khoshaghideh F, Lee S, Lee SJ. Impairment of microtubule-dependent trafficking by overexpression of alpha-synuclein. The European journal of neuroscience. 2006; 24:3153–3162. [PubMed: 17156376]

Liu S, Sawada T, Lee S, et al. Parkinson's disease-associated kinase PINK1 regulates Miro protein level and axonal transport of mitochondria. PLoS genetics. 2012; 8:e1002537. [PubMed: 22396657]

Lopes FM, Schroder R, da Frota ML Jr, et al. Comparison between proliferative and neuron-like SH-SY5Y cells as an in vitro model for Parkinson disease studies. Brain research. 2010; 1337:85–94. [PubMed: 20380819]

Luduena RF, Roach MC. Tubulin sulfhydryl groups as probes and targets for antimitotic and antimicrotubule agents. Pharmacology & therapeutics. 1991; 49:133–152. [PubMed: 1852786]

Mandir AS, Przedborski S, Jackson-Lewis V, et al. Poly(ADP-ribose) polymerase activation mediates 1-methyl-4-phenyl-1, 2,3,6-tetrahydropyridine (MPTP)-induced parkinsonism. Proceedings of the National Academy of Sciences of the United States of America. 1999; 96:5774–5779. [PubMed: 10318960]

Matov A, Applegate K, Kumar P, et al. Analysis of microtubule dynamic instability using a plus-end growth marker. Nature methods. 2010; 7:761–768. [PubMed: 20729842]

Meijering E, Dzyubachyk O, Smal I. Methods for cell and particle tracking. Methods in enzymology. 2012; 504:183–200. [PubMed: 22264535]

Mellon MG, Rebhun LI. Sulfhydryls and the in vitro polymerization of tubulin. The Journal of cell biology. 1976; 70:226–238. [PubMed: 945278]

Michan S, Sinclair D. Sirtuins in mammals: insights into their biological function. The Biochemical journal. 2007; 404:1–13. [PubMed: 17447894]

Morfini G, Pigino G, Opalach K, et al. 1-Methyl-4-phenylpyridinium affects fast axonal transport by activation of caspase and protein kinase C. Proceedings of the National Academy of Sciences of the United States of America. 2007; 104:2442–2447. [PubMed: 17287338]

Morfini GA, Burns M, Binder LI, et al. Axonal transport defects in neurodegenerative diseases. The Journal of neuroscience : the official journal of the Society for Neuroscience. 2009; 29:12776–12786. [PubMed: 19828789]

Nakabeppu Y, Tsuchimoto D, Yamaguchi H, Sakumi K. Oxidative damage in nucleic acids and Parkinson's disease. Journal of neuroscience research. 2007; 85:919–934. [PubMed: 17279544]

North BJ, Marshall BL, Borra MT, Denu JM, Verdin E. The human Sir2 ortholog, SIRT2, is an NAD +-dependent tubulin deacetylase. Molecular cell. 2003; 11:437–444. [PubMed: 12620231]

North BJ, Verdin E. Interphase nucleo-cytoplasmic shuttling and localization of SIRT2 during mitosis. PloS one. 2007; 2:e784. [PubMed: 17726514]

Pandithage R, Lilischkis R, Harting K, et al. The regulation of SIRT2 function by cyclin-dependent kinases affects cell motility. The Journal of cell biology. 2008; 180:915–929. [PubMed: 18332217]

Patel M, Day BJ. Metalloporphyrin class of therapeutic catalytic antioxidants. Trends in pharmacological sciences. 1999; 20:359–364. [PubMed: 10462758]

Patel VP, Defranco DB, Chu CT. Altered transcription factor trafficking in oxidatively-stressed neuronal cells. Biochimica et biophysica acta. 2012; 1822:1773–1782. [PubMed: 22902725]

Pham NA, Richardson T, Cameron J, Chue B, Robinson BH. Altered mitochondrial structure and motion dynamics in living cells with energy metabolism defects revealed by real time microscope imaging. Microscopy and microanalysis : the official journal of Microscopy Society of America, Microbeam Analysis Society, Microscopical Society of Canada. 2004; 10:247–260.

Pittelli M, Felici R, Pitozzi V, et al. Pharmacological effects of exogenous NAD on mitochondrial bioenergetics, DNA repair, and apoptosis. Molecular pharmacology. 2011; 80:1136–1146. [PubMed: 21917911]

Pollak N, Niere M, Ziegler M. NAD kinase levels control the NADPH concentration in human cells. The Journal of biological chemistry. 2007; 282:33562–33571. [PubMed: 17855339]

Przedborski S, Ischiropoulos H. Reactive oxygen and nitrogen species: weapons of neuronal destruction in models of Parkinson's disease. Antioxidants & redox signaling. 2005; 7:685–693. [PubMed: 15890013]

Ross CA, Smith WW. Gene-environment interactions in Parkinson's disease. Parkinsonism & related disorders. 2007; 13(Suppl 3):S309–315. [PubMed: 18267256]

Rouleau M, Patel A, Hendzel MJ, Kaufmann SH, Poirier GG. PARP inhibition: PARP1 and beyond. Nature reviews Cancer. 2010; 10:293–301.

Saha AR, Hill J, Utton MA, et al. Parkinson's disease alpha-synuclein mutations exhibit defective axonal transport in cultured neurons. Journal of cell science. 2004; 117:1017–1024. [PubMed: 14996933]

Singh R, Mailloux RJ, Puiseux-Dao S, Appanna VD. Oxidative stress evokes a metabolic adaptation that favors increased NADPH synthesis and decreased NADH production in Pseudomonas fluorescens. Journal of bacteriology. 2007; 189:6665–6675. [PubMed: 17573472]

Smyth JW, Hong TT, Gao D, et al. Limited forward trafficking of connexin 43 reduces cell-cell coupling in stressed human and mouse myocardium. The Journal of clinical investigation. 2010; 120:266–279. [PubMed: 20038810]

Stepanova T, Slemmer J, Hoogenraad CC, et al. Visualization of microtubule growth in cultured neurons via the use of EB3-GFP (end-binding protein 3-green fluorescent protein). The Journal of neuroscience : the official journal of the Society for Neuroscience. 2003; 23:2655–2664. [PubMed: 12684451]

Sudo H, Baas PW. Acetylation of microtubules influences their sensitivity to severing by katanin in neurons and fibroblasts. The Journal of neuroscience : the official journal of the Society for Neuroscience. 2010; 30:7215–7226. [PubMed: 20505088]

Tan EK, Skipper LM. Pathogenic mutations in Parkinson disease. Human mutation. 2007; 28:641–653. [PubMed: 17385668]

Terzioglu M, Galter D. Parkinson's disease: genetic versus toxin-induced rodent models. The FEBS journal. 2008; 275:1384–1391. [PubMed: 18279376]

Tirnauer JS, Grego S, Salmon ED, Mitchison TJ. EB1-microtubule interactions in Xenopus egg extracts: role of EB1 in microtubule stabilization and mechanisms of targeting to microtubules. Molecular biology of the cell. 2002; 13:3614–3626. [PubMed: 12388761]

Tran AD, Marmo TP, Salam AA, et al. HDAC6 deacetylation of tubulin modulates dynamics of cellular adhesions. Journal of cell science. 2007; 120:1469–1479. [PubMed: 17389687]

Ursini MV, Parrella A, Rosa G, Salzano S, Martini G. Enhanced expression of glucose-6-phosphate dehydrogenase in human cells sustaining oxidative stress. The Biochemical journal. 1997; 323(Pt 3):801–806. [PubMed: 9169615]

van der Vaart B, Akhmanova A, Straube A. Regulation of microtubule dynamic instability. Biochemical Society transactions. 2009; 37:1007–1013. [PubMed: 19754441]

Vasiliou V, Nebert DW. Analysis and update of the human aldehyde dehydrogenase (ALDH) gene family. Human genomics. 2005; 2:138–143. [PubMed: 16004729]

Verdel A, Curtet S, Brocard MP, et al. Active maintenance of mHDA2/mHDAC6 histone-deacetylase in the cytoplasm. Current biology : CB. 2000; 10:747–749. [PubMed: 10873806]

Virag L, Szabo C. The therapeutic potential of poly(ADP-ribose) polymerase inhibitors. Pharmacological reviews. 2002; 54:375–429. [PubMed: 12223530]

Xie HR, Hu LS, Li GY. SH-SY5Y human neuroblastoma cell line: in vitro cell model of dopaminergic neurons in Parkinson's disease. Chinese medical journal. 2010; 123:1086–1092. [PubMed: 20497720]

Yang SR, Chida AS, Bauter MR, et al. Cigarette smoke induces proinflammatory cytokine release by activation of NF-kappaB and posttranslational modifications of histone deacetylase in macrophages. American journal of physiology. Lung cellular and molecular physiology. 2006; 291:L46–57. [PubMed: 16473865]

Yang Y, Fu W, Chen J, et al. SIRT1 sumoylation regulates its deacetylase activity and cellular response to genotoxic stress. Nature cell biology. 2007; 9:1253–1262.

Ying W. NAD+/NADH and NADP+/NADPH in cellular functions and cell death: regulation and biological consequences. Antioxidants & redox signaling. 2008; 10:179–206. [PubMed: 18020963]

Yoritaka A, Hattori N, Uchida K, Tanaka M, Stadtman ER, Mizuno Y. Immunohistochemical detection of 4-hydroxynonenal protein adducts in Parkinson disease. Proceedings of the National Academy of Sciences of the United States of America. 1996; 93:2696–2701. [PubMed: 8610103]

Zee RS, Yoo CB, Pimentel DR, et al. Redox regulation of sirtuin-1 by S-glutathiolation. Antioxidants & redox signaling. 2010; 13:1023–1032. [PubMed: 20392170]

Zhu JH, Horbinski C, Guo F, Watkins S, Uchiyama Y, Chu CT. Regulation of autophagy by extracellular signal-regulated protein kinases during 1-methyl-4-phenylpyridinium-induced cell death. The American journal of pathology. 2007; 170:75–86. [PubMed: 17200184]

Zhu JH, Kulich SM, Oury TD, Chu CT. Cytoplasmic aggregates of phosphorylated extracellular signal-regulated protein kinases in Lewy body diseases. The American journal of pathology. 2002; 161:2087–2098. [PubMed: 12466125]

Highlights

- We employed the oxidative parkinsonian neurotoxin, 6-hydroxydopamine (6OHDA)
- 6OHDA elicited significant alterations in microtubule (MT) dynamics
- 6OHDA decreased SIRT2 function, resulting in increased tubulin acetylation
- Restoration of SIRT2 function rescued MT dynamics and reduced neurite shortening

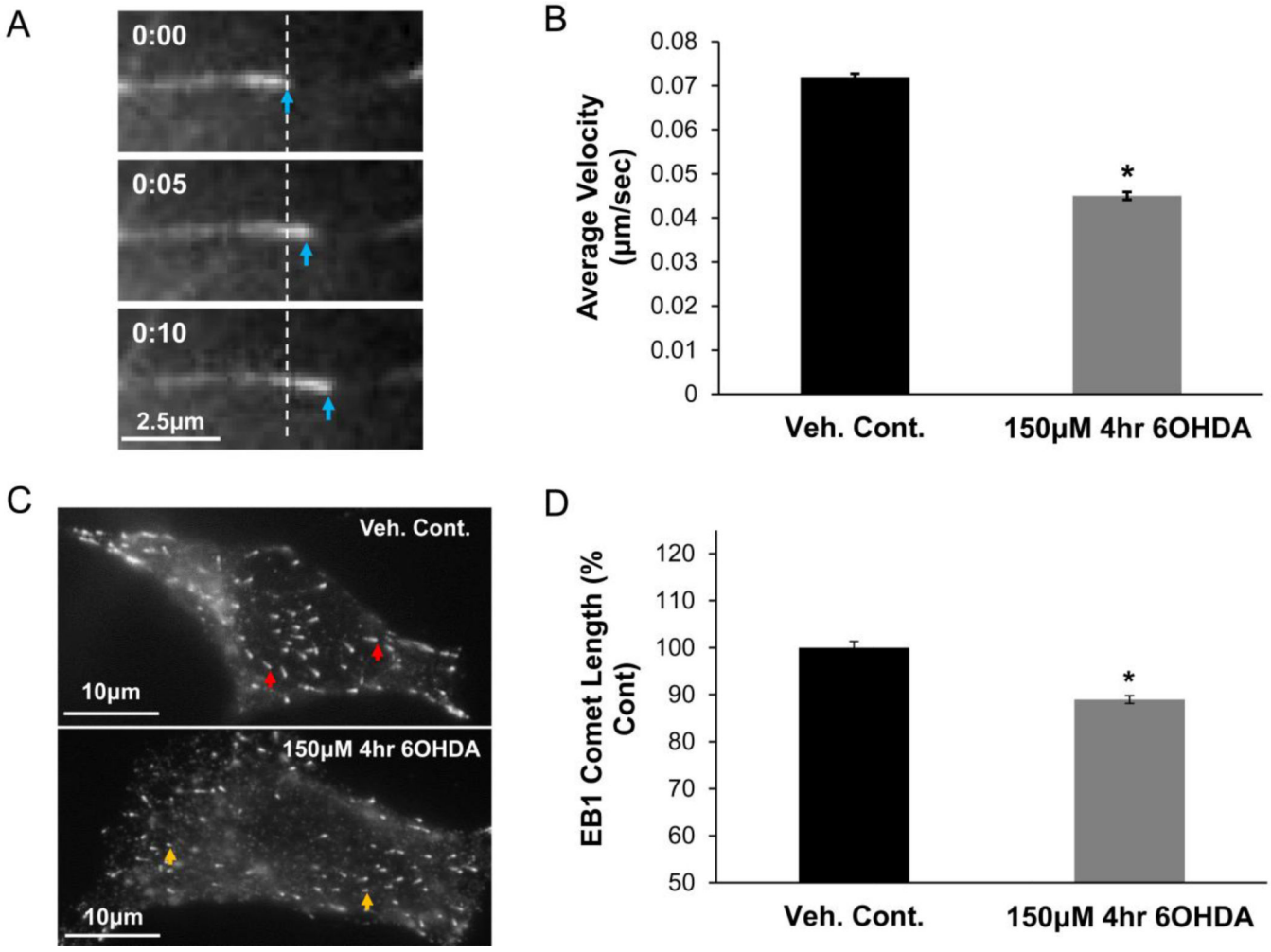

Figure 1. Pre-lethal 6OHDA reduces MT growth rate

(A) SH-SY5Y cells were transfected with an expression plasmid for EB3-GFP. The EB3-GFP comet is seen moving with time. (B) SH-SY5Y cells expressing EB3-GFP were treated with 150μM 6OHDA for 4hr (a pre-lethal dose), which led to a significant reduction in MT growth rate. Mean +/− SEM, **p* < 0.05 vs. Veh. Cont. *n* = 150 – 200 EB3-GFP comets per condition. (C & D) SH-SY5Y cells treated with vehicle or a pre-lethal dose of 6OHDA were fixed and immunostained for endogenous EB1. Representative images (C) and quantification (D) show reduced comet length with 6OHDA treatment. Mean +/−SEM, **p* < 0.05 vs. Veh. Cont. *n* = 200 – 300 EB1 comets per condition.

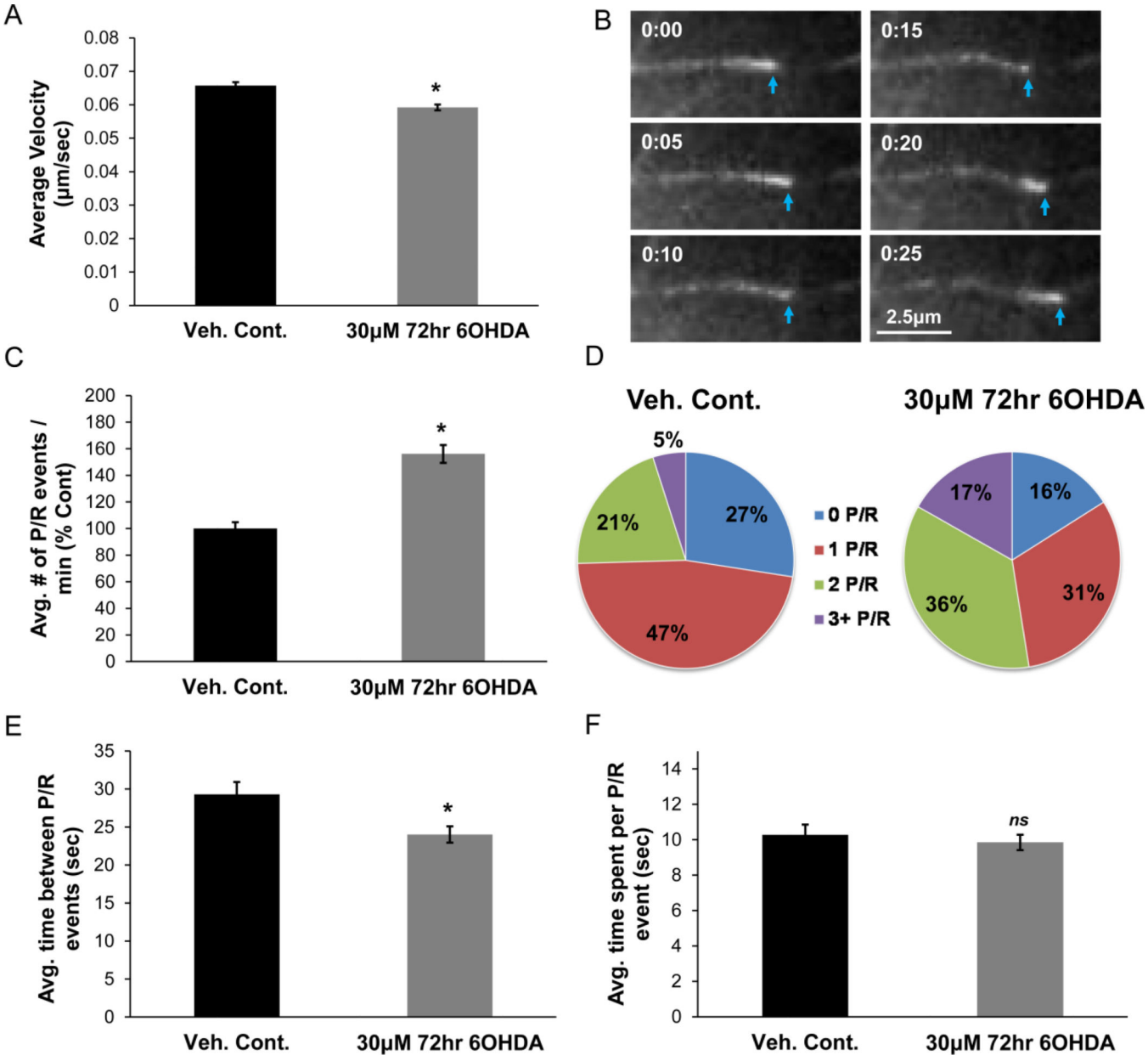

Figure 2. Sub-lethal 6OHDA alters MT dynamics

(A) Differentiated SH-SY5Y cells expressing EB3-GFP were treated with 30μM 6OHDA for 72hr (treatment every 24hr). MTs along the length of the neurite in 6OHDA-treated cells show reduced growth rates. Mean +/− SEM, **p* < 0.05 vs. Veh. Cont. *n* = 150 – 200 EB3-GFP comets per condition. (B) An example of a "dimming" event where the EB3-GFP comet loses its fluorescent intensity (0:10 to 0:15), suggesting MT pausing or retraction. Return to growth phase is noted by the increase in the fluorescent intensity and the forward movement of the comet. (C) An increase in the frequency of MT pauses and/or retractions (P/R) was seen after sub-lethal 6OHDA treatment. Mean +/− SEM, **p* < 0.05 vs. Veh. Cont. *n* = 100 – 200 EB3-GFP comets per condition. (D) An increase in the percentage of MTs with 2 and 3+ P/R events and a reduction in the percentage of MTs with 0 and 1 P/R event

was observed. (E & F) The average amount of time between two P/R events is reduced with treatment (E); however the amount of time spent in an individual P/R event is not altered (F). Mean +/− SEM, $*p < 0.05$ or $^{ns}p > 0.05$ vs. Veh. Cont. $n = 100 – 200$ EB3-GFP comets per condition.

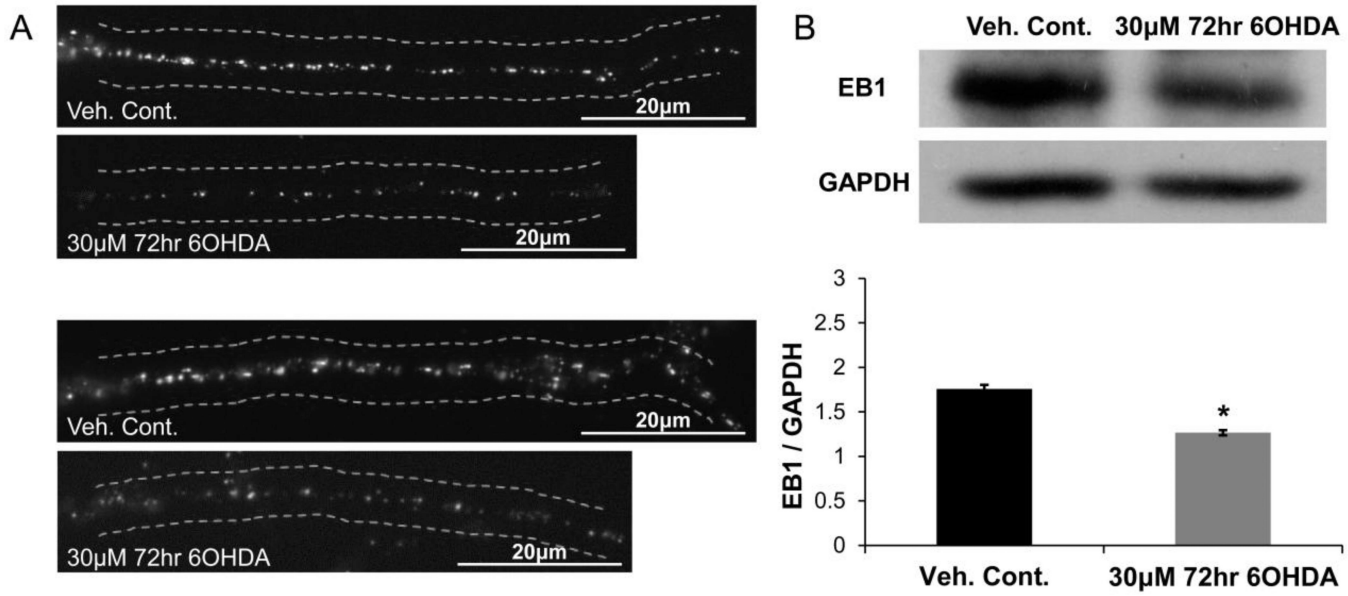

Figure 3. Sub-lethal 6OHDA reduces EB1 levels

SH-SY5Y cells were treated with sub-lethal 6OHDA and EB1 levels were analyzed via immunocytochemistry and Western blotting. (A) Two sets of representative images are shown where reduced EB1 staining is noted along the length of the neurite in 6OHDA-treated cells. (B) Western blot of total cellular EB1 levels showed a reduction with 6OHDA treatment. Mean +/− SEM, *$p < 0.05$ vs. Veh. Cont.

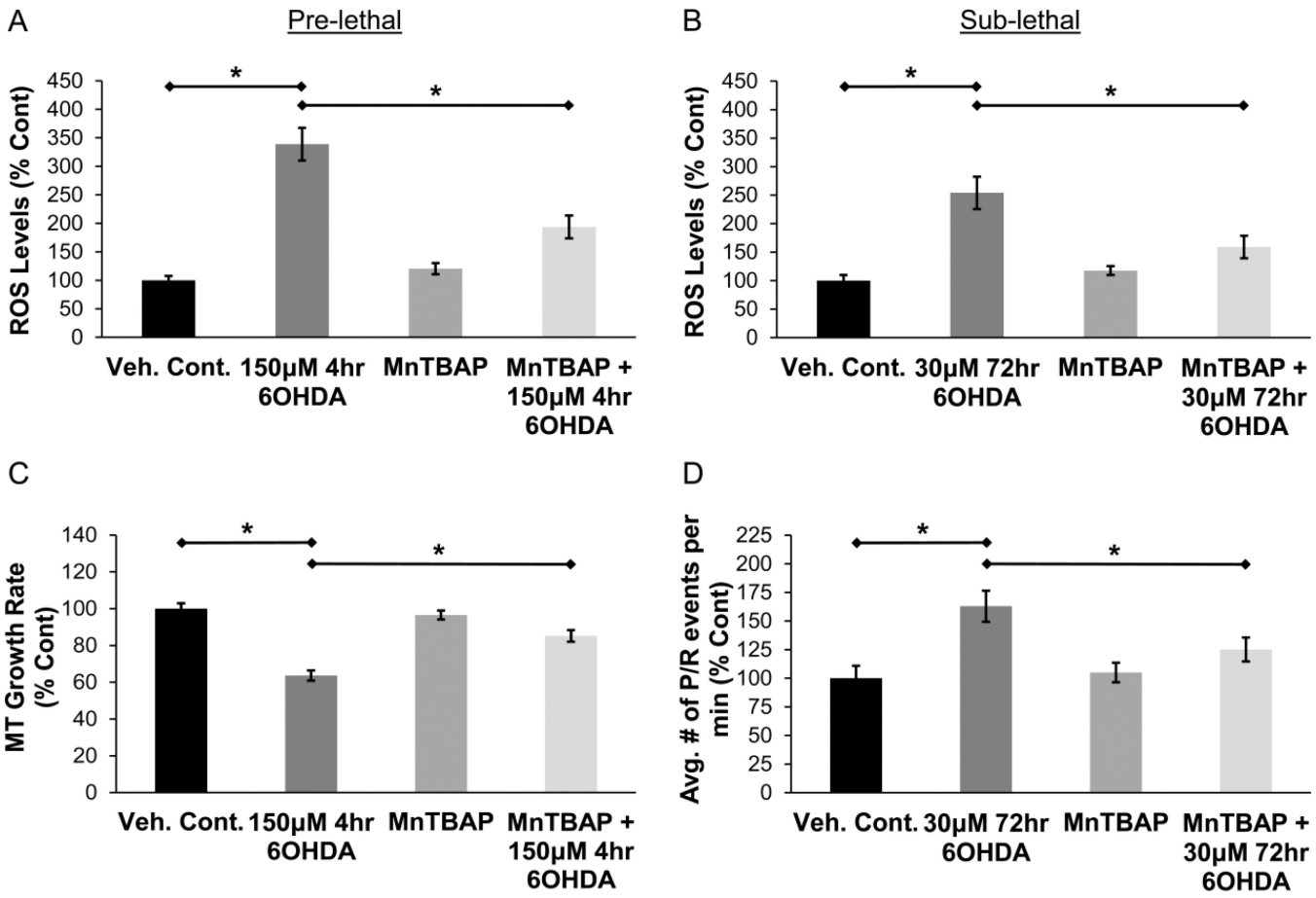

Figure 4. 6OHDA increases ROS levels and antioxidant treatment rescues 6OHDA-induced impairments in MT dynamics

(A & B) Pre-lethal and sub-lethal 6OHDA increase ROS levels in SH-SY5Y cells, which are reduced by pre-treatment with an antioxidant, MnTBAP. Cells were treated with 200μM MnTBAP 30min prior to pre-lethal 6OHDA injury (A) or 30μM MnTBAP 30min prior to sub-lethal 6OHDA injury (B). Mean +/− SEM, *$p < 0.05$ as indicated. (C) SH-SY5Y cells expressing EB3-GFP were pre-treated with 200μM MnTBAP for 30min and then treated with pre-lethal 6OHDA. Rescue of MT growth rate was observed in cells pre-treated with MnTBAP. Mean +/− SEM, *$p < 0.05$ as indicated. $n = 75 – 100$ EB3-GFP comets per condition. (D) SH-SY5Y cells expressing EB3-GFP were pre-treated with 30μM MnTBAP for 30min and then treated with sub-lethal 6OHDA. Increase in the frequency of pauses / retractions after 6OHDA injury was significantly reduced in cells pre-treated with MnTBAP. Mean +/− SEM, *$p < 0.05$ as indicated. $n = 75 – 100$ EB3-GFP comets per condition.

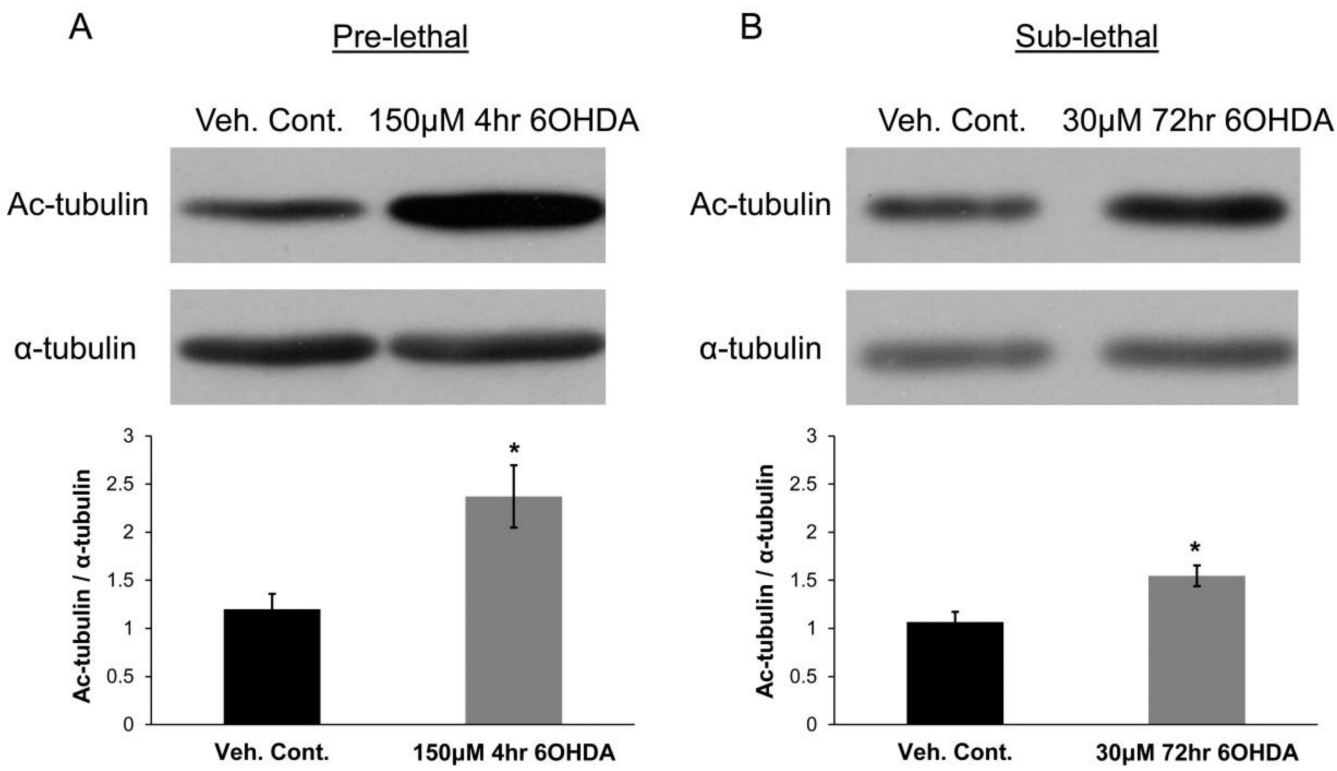

Figure 5. 6OHDA increases MT acetylation

SH-SY5Y cells were treated with pre-lethal (A) or sub-lethal (B) 6OHDA and levels of tubulin acetylation were examined via Western blot analysis. A significant increase in tubulin acetylation was observed in treated cells. Mean +/− SEM, *$p < 0.05$ vs. Veh. Cont.

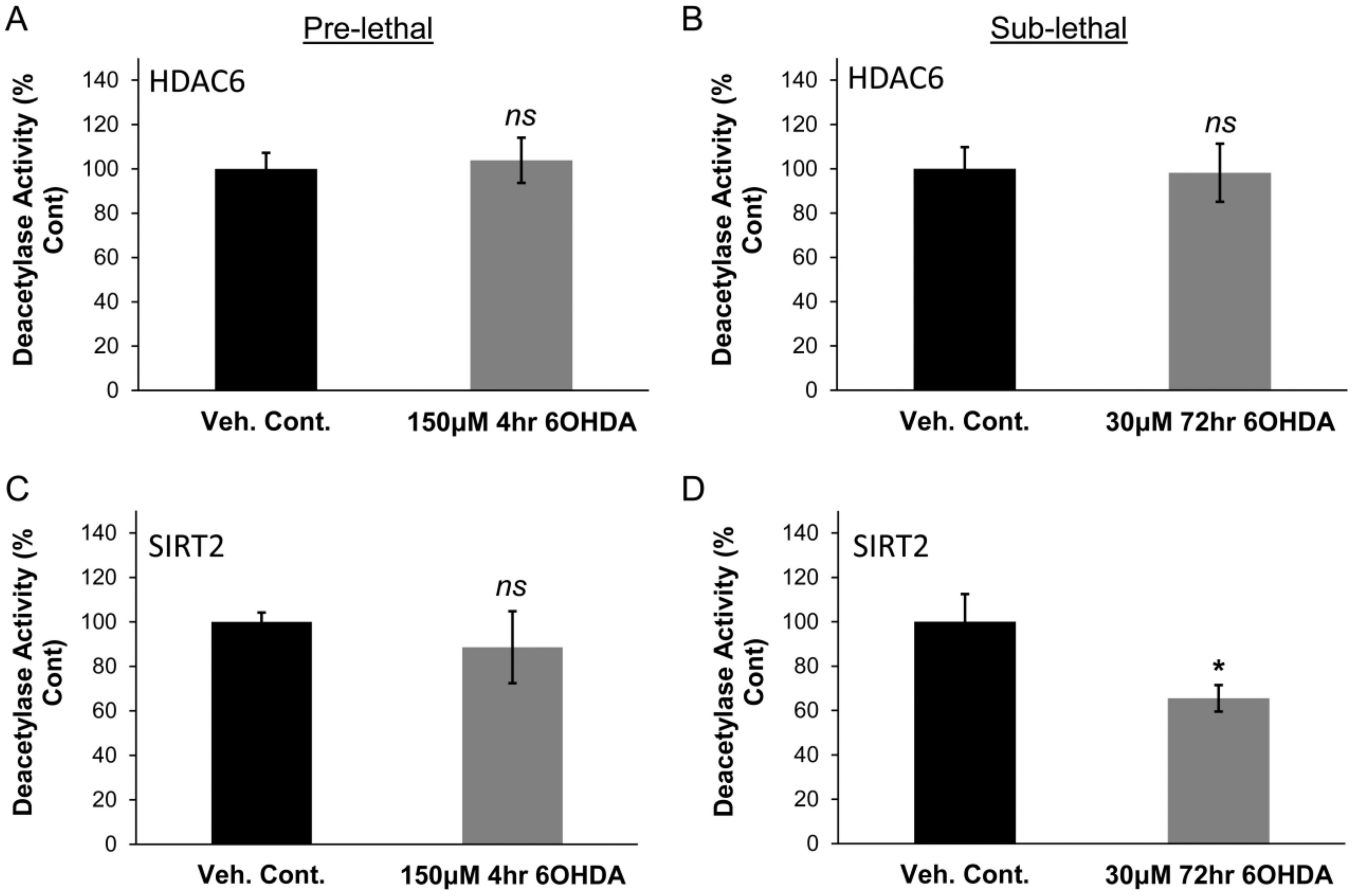

Figure 6. Sub-lethal 6OHDA reduces SIRT2 deacetylase activity

SH-SY5Y cells were treated with either pre-lethal (A & C) or sub-lethal (B & D) 6OHDA and the deacetylase activity of the pulled-down enzyme was examined. (A & B) No significant change in enzymatic activity of HDAC6 was observed. Mean +/− SEM, $^{ns}p > 0.05$ vs. Veh. Cont. (C & D) Pre-lethal 6OHDA did not reduce SIRT2 activity (C); however a reduction was observed after sub-lethal 6OHDA treatment (D). Mean +/− SEM, $*p < 0.05$ or $^{ns}p > 0.05$ vs. Veh. Cont.

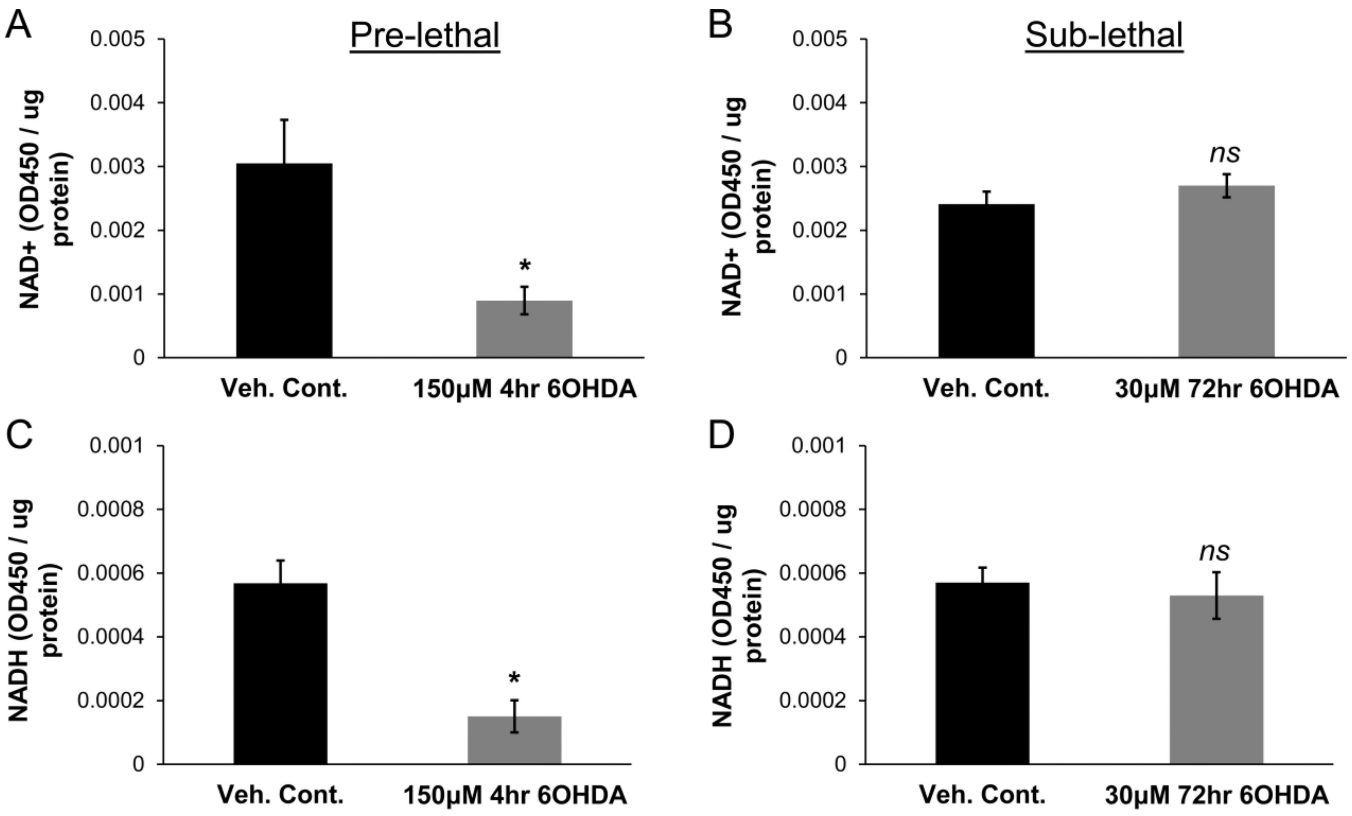

Figure 7. Pre-lethal but not sub-lethal 6OHDA reduces NAD+ and NADH levels

SH-SY5Y cells were treated with either pre-lethal (A & C) or sub-lethal (B & D) 6OHDA. NAD+ and NADH levels were determined via an enzyme cycling reaction and the levels were normalized to total protein. (A & C) Significant reduction in both NAD+ and NADH levels was observed after pre-lethal injury. Mean +/− SEM, $*p < 0.05$ vs. Veh. Cont. (B & D) No reduction in levels of either NAD+ or NADH was observed after sub-lethal injury. Mean +/− SEM, $^{ns}p > 0.05$ vs. Veh. Cont.

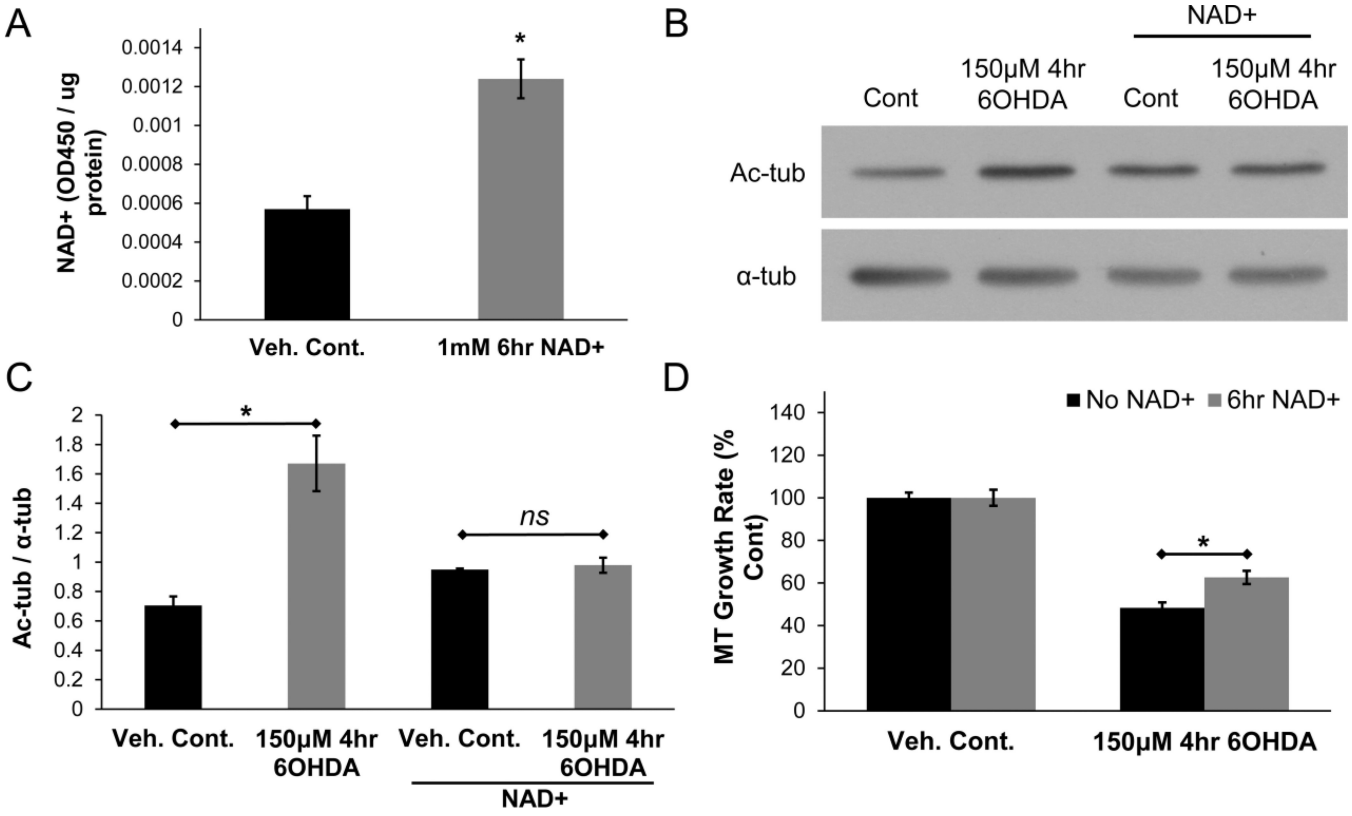

Figure 8. NAD+ rescues tubulin acetylation levels and improves MT growth rate

(A) Treatment of SH-SY5Y cells with 1mM NAD+ for 6hr led to an increase in intracellular NAD+ levels. Mean +/− SEM, *$p < 0.05$ vs. Veh. Cont. (B & C) Pre-treatment of cells with NAD+ (1mM; 6hr) prevented the 6OHDA-mediated increase in tubulin acetylation levels. Mean +/− SEM, *$p < 0.05$ or $^{ns}p > 0.05$ as indicated. (D) Pre-treatment with NAD+ reduced the impairment in MT growth rate caused by pre-lethal 6OHDA. Mean +/− SEM, *$p < 0.05$ as indicated. $n = 75 – 100$ EB3-mCherry comets per condition.

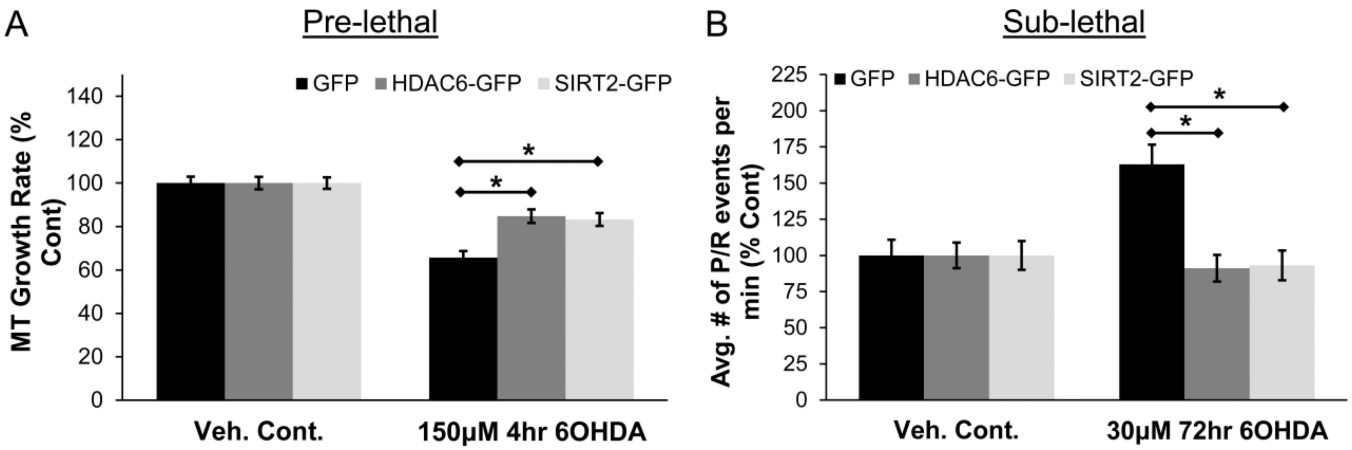

Figure 9. HDAC6 and SIRT2 overexpression rescues MT dynamics

(A) SH-SY5Y cells expressing EB3-mCherry and either GFP, HDAC6-GFP, or SIRT2-GFP were treated with pre-lethal 6OHDA and MT growth rate was determined. Rescue was observed in cells overexpressing HDAC6-GFP or SIRT2-GFP. Mean +/− SEM, *$p < 0.05$ as indicated. $n = 75 – 100$ EB3-mCherry comets per condition. (B) Frequency of pauses / retractions was determined in cells treated with sub-lethal 6OHDA. Increase in the frequency of these events was reversed by the overexpression of either HDAC6-GFP or SIRT2-GFP. Mean +/− SEM, *$p < 0.05$ as indicated. $n = 75 – 100$ EB3-mCherry comets per condition.

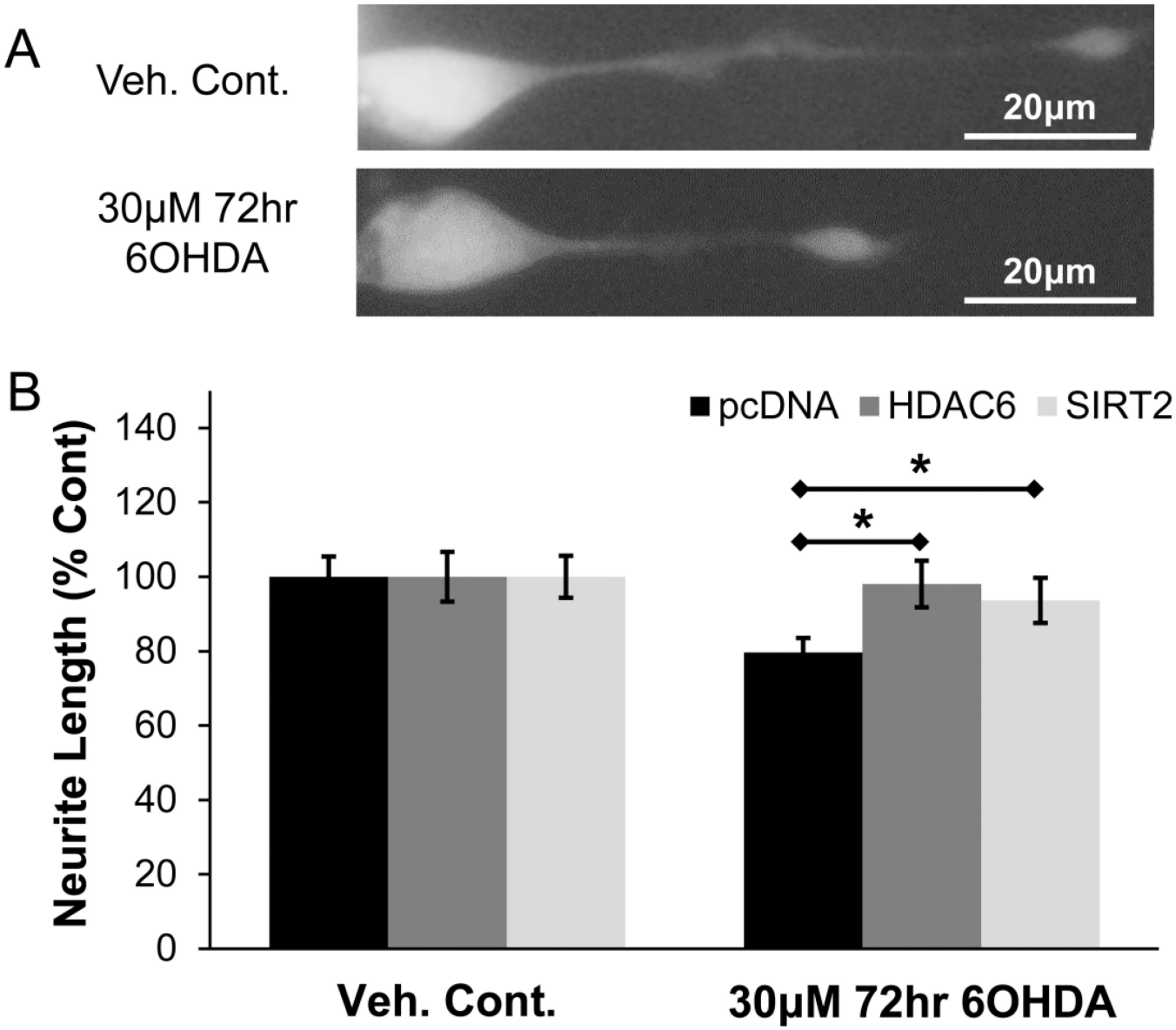

Figure 10. HDAC6 and SIRT2 rescue 6OHDA-mediated reduction in neurite length

(A) Differentiated SH-SY5Y cells transfected with GFP and treated with sub-lethal 6OHDA. Representative images show reduced length of the neurite. (B) Cells expressing GFP and either pcDNA, HDAC6-FLAG, or SIRT2-FLAG were treated with sub-lethal 6OHDA. HDAC6 and SIRT2 were detected by FLAG immunofluorescence. Rescue in neurite length was observed with either HDAC6 or SIRT2 overexpression. Mean +/− SEM, *$p < 0.05$ as indicated. $n = 150 – 200$ cells per condition.